

ARTICLE

Received 5 May 2014 | Accepted 12 Nov 2014 | Published 19 Dec 2014

DOI: 10.1038/ncomms6833

Arabidopsis ERF109 mediates cross-talk between jasmonic acid and auxin biosynthesis during lateral root formation

Xiao-Teng Cai¹, Ping Xu¹, Ping-Xia Zhao¹, Rui Liu¹, Lin-Hui Yu¹ & Cheng-Bin Xiang¹

Jasmonic acid (JA) is well known to promote lateral root formation but the mechanisms by which JA signalling is integrated into the pathways responsible for lateral root formation, and how it interacts with auxin in this process remains poorly understood. Here, we report that the highly JA-responsive ethylene response factor 109 (ERF109) mediates cross-talk between JA signalling and auxin biosynthesis to regulate lateral root formation in *Arabidopsis*. *erf109* mutants have fewer lateral roots under MeJA treatments compared with wild type whereas *ERF109* overexpression causes a root phenotype that resembles those of auxin overproduction mutants. ERF109 binds directly to GCC-boxes in the promoters of *ASA1* and *YUC2*, which encode two key enzymes in auxin biosynthesis. Thus, our study reveals a molecular mechanism for JA and auxin cross-talk during JA-induced lateral root formation.

¹School of Life Sciences, University of Science and Technology of China, Hefei 230027, China. Correspondence and requests for materials should be addressed to C.-B.X. (email: xiangcb@ustc.edu.cn).

Improved root architecture is crucial for crop productivity and a very important contributor to drought resistance¹. Most dicotyledonous plants have tap root systems, whereas monocotyledonous plants have fibrous root systems composed of adventitious roots (AR)². Primary root (PR) development starts during embryogenesis. Lateral root (LR) development is initiated from asymmetric divisions of the pericycle founder cell of PR and the whole process of development has been well established^{3,4}.

It is well known that the phytohormone auxin has a very important role in root development⁵. It is involved in every stage of LR formation^{5,6}. Auxin biosynthesis, transport and auxin-dependent signalling processes all affect LR formation^{7–9}. In *Arabidopsis* roots, an elevated auxin level causes the degradation of indole-3-acetic acid/auxin (IAA/AUX) and increases the levels of auxin response factors (ARFs)^{10,11}. ARFs activate the functions of lateral organ boundaries-domain (LBD) to promote LR formation and enhance LR density^{12,13}. Mutations in the genes involved in auxin biosynthesis, transport and signalling greatly impact LR initiation and formation^{3,6}. Auxin overproduction mutants, such as the gain-of-function *yucca* mutant, *superroot1* (*sur1*), *sur2* and *arf8*, increase LR number^{3,14}. The mutants with defects in auxin transport, such as *auxin resistant 1* (*aux1*), *like aux1 3* (*lax3*), *pin-formed* (*pin*) multiple mutants, *gnom* and *auxin resistant 4* (*axr4*), have reduced LR number or aberrant lateral root primordium (LRP)³. Auxin signalling mutants, including *arf7 arf19* double mutants, gain-of-function *iaa14/solitaryroot 1* (*slr1*) mutant, gain-of-function *iaa19/massugu 2* (*msg2*) mutant, gain-of-function *iaa28* mutant and *lbd16 lbd18* double mutants, show severe damage or complete absence of LR formation^{3,5}.

Interactions among plant hormones form a complex network to regulate developmental processes^{15,16}. In most cases, other hormones regulate root development through the interaction with auxin^{6,17}. Among these hormones, the functions of jasmonic acid (JA) in wounding and defence responses of plants were well studied and its roles in plant growth and development were also reported^{18,19}. With exogenous JA treatments, plants showed short PRs and more LRs²⁰. Interactions of JA with other hormones have been reported²¹. JA and auxin share some signalling pathway components^{22–24}. These two plant hormones have demonstrated cross-talk through the action of ARFs²⁵. In addition, JA signalling pathway is linked to auxin homeostasis through the modulation of *YUCCA8* (*YUC8*) and *YUC9* gene expressions^{26,27}. *Anthranilate synthase alpha subunit 1* (*ASA1*, At5g05730), which encodes an L-tryptophan (Trp) biosynthesis enzyme, mediates JA-induced auxin accumulation and transport²⁸. The transcription levels of several genes involved in auxin biosynthesis are also upregulated by methyl jasmonate (MeJA)²⁸. Among these genes, *YUC2* (At4g13260) encodes a flavin monooxygenase-like enzyme, which catalyses a rate-limiting step in Trp-dependent auxin biosynthesis pathway with functional redundancy of *YUCCA* family^{14,29}. Furthermore, JA was reported to affect auxin transport³⁰. Despite the recent progress, the molecular mechanisms underlying the interaction between JA and IAA are far from being well understood.

The *Arabidopsis* mutant *enhanced drought tolerance 1* (*edt1*) showed improved drought tolerance with a more extensive root system, which was caused by the strong expression of the homeodomain transcription factor *homeodomain glabrous 11* (*HDG11*) in a constitutive fashion³¹. To study the molecular mechanisms of improved root architecture of *edt1*, the root transcriptomes of *edt1* and the wild type were compared. We found that a transcription factor named ethylene response factor 109 (*ERF109*) (At4g34410) was remarkably upregulated in the roots of *edt1* seedlings. *ERF109* encodes a plant specific

transcription factor of the *ERF* family, which contains only one APETALA2 (AP2) domain responsible for binding to the promoters of downstream target genes^{32–34}. ERFs are also named as ethylene-responsive element binding proteins (EREBPs), which were first identified in tobacco and found to directly bind to the *cis*-element called a GCC-box containing the core 5'-GCCGCC-3' sequence³². The transcription of *ERF109* is inducible by MeJA treatment³⁵. In addition, *ERF109* was reportedly expressed during the re-adjustment of *Arabidopsis* leaves to homeostasis after high light stress, and consequently named *redox-responsive transcription factor 1* (ref. 36).

Here, we report that *AtERF109* integrates JA signalling into auxin pathways to regulate root architecture. Although it is very weakly expressed under normal growth conditions, *ERF109* is highly responsive to MeJA treatment in *Arabidopsis* roots. Genetic analysis with *ERF109* knockout mutants and overexpression lines demonstrates that *ERF109* regulates LRP development and JA-induced LR formation. The *ERF109* overexpression lines (*35S-ERF109*) show shorter PR, increased number of LRP, enhanced LR density and other phenotypes typical of those caused by elevated auxin levels. We also find that *ERF109* binds directly to the promoters of *ASA1* and *YUC2*, which encode key enzymes in auxin biosynthesis pathways.

Results

***ERF109* is highly responsive to MeJA.** JA-induced expression of *ERF109* was analysed in a time course. *ERF109* was transiently upregulated by MeJA treatments. The transcript level of *ERF109* peaked with a 20-fold induction at 20 min and was restored to the previous level at 1 h after MeJA treatment, which is in agreement with the previous report (Fig. 1a)³⁵.

The responses of *ERF109* to different hormones and stresses were analysed using β -glucuronidase (GUS) staining and quantitative PCR with reverse transcription (RT-PCR) subsequently (Supplementary Fig. 1). The GUS staining was significantly induced by MeJA and weakly induced by salicylic acid (SA) and 1-aminocyclopropane-1-carboxylic acid (ACC) (Supplementary Fig. 1a–d), but apparently not by abscisic acid (ABA), gibberellin (GA), IAA or 6-benzylaminopurine (6-BA) treatments (Supplementary Fig. 1e–h). Interestingly, the expression of *ERF109* was also weakly induced by NaCl and paraquat (PQ) treatments (Supplementary Fig. 1i,k). The quantitative RT-PCR results are consistent with the GUS staining for MeJA, SA, ACC, IAA, 6-BA, NaCl, mannitol and PQ treatments, but not for ABA and GA that slightly induced the expression of *ERF109* (Supplementary Fig. 1l). In addition, no significant difference was found during the salt-induced adventitious root formation (Supplementary Fig. 1m–o).

Under normal conditions, *ERF109* was expressed in all tissues examined but at low levels in roots as demonstrated by quantitative RT-PCR and *ERF109pro-GUS* reporter analyses (Supplementary Fig. 2). However, in the *coronatine insensitive 1* (*coi1*) background, MeJA-induced expression of *ERF109* was abolished, which is in agreement with a previous report (Fig. 1b)³⁵. This result indicates that MeJA-induction of *ERF109* requires the function of COI1, the receptor of JA-isoleucine (Ile) in *Arabidopsis*^{35,37–39}. Therefore, *ERF109* is under the regulation of JA signalling.

To study the spatial pattern of *ERF109* in response to JA treatments, we treated the *ERF109pro-GUS* reporter lines with MeJA for 0.5 h. The GUS staining results showed that under normal conditions, *ERF109* was very weakly expressed only in the tip and base of LRs in the roots (Fig. 1c–i). However, in response to MeJA treatment, the expression of *ERF109* was dramatically induced in both shoots and roots, especially in the region behind

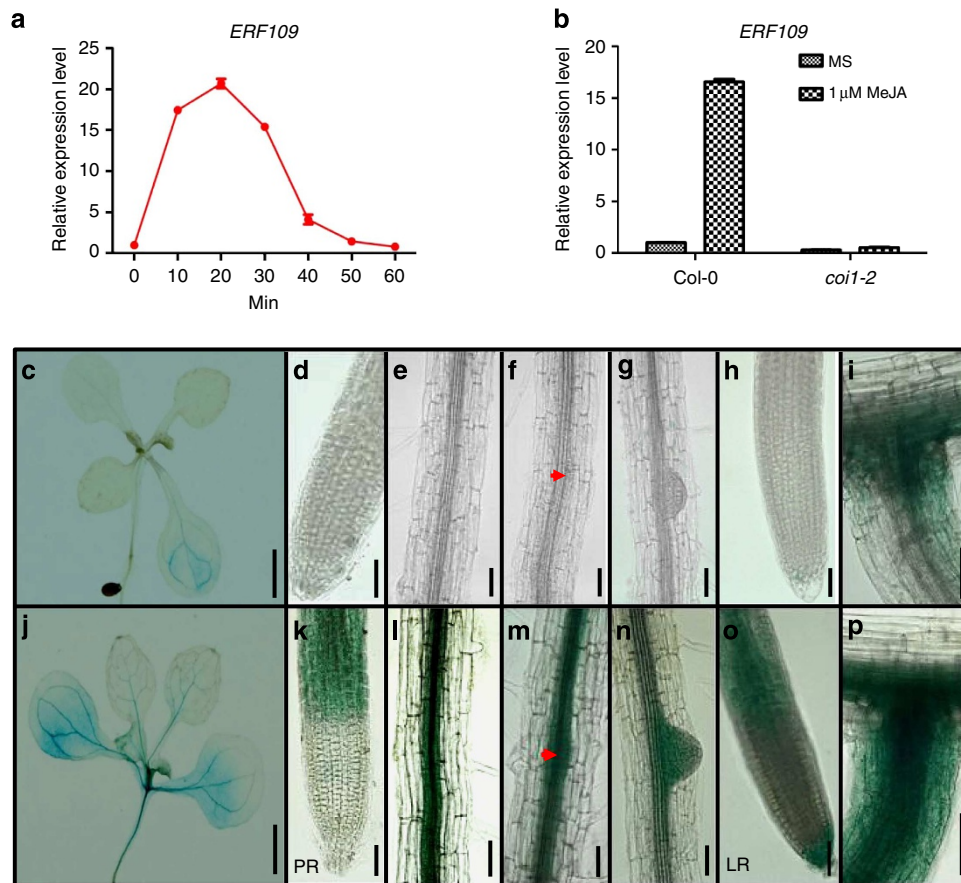


Figure 1 | *ERF109* is highly responsive to MeJA. (a) *ERF109* is transiently induced by MeJA. The time course analysis of *ERF109* expression in response to MeJA treatment was conducted. Col-0 seedlings were grown on MS medium vertically for 14 days. Then, the seedlings were transferred to MS medium without (control) or with 1 μ M MeJA for the indicated times before RNA extraction. RNA was isolated at indicated time points and quantitative RT-PCR analysis was performed subsequently. Values are mean \pm s.d. ($n = 3$ experiments). (b) MeJA-induced expression of *ERF109* requires the function of COI1. The 14-day-old Col-0 and *coi1-2* seedlings were treated with 1 μ M of MeJA for 0.5 h. Then RNA was isolated and quantitative RT-PCR analysis was performed. Values are mean \pm s.d. ($n = 3$ experiments). (c-i) GUS staining of 7-day-old transgenic lines contained *ERF109pro-GUS* without MeJA treatment. GUS expressions in cotyledon (c), primary root (d), stele (e), LRP at all developmental stages (f and g) and the tip and base of LR (h and i). (c) Scale bar, 1 mm; (d-i) Scale bars, 50 μ m. (j-p) GUS staining of 7-day-old transgenic lines contained *ERF109pro-GUS* with 10 μ M MeJA treatment for 0.5 h. GUS expressions were significantly enhanced in cotyledon (j), primary root (k), stele (l), LRP at all developmental stages (m and n) and the tip and base of LR (o and p). (j) Scale bar, 1 mm; (k-p) Scale bars, 50 μ m. The locations of LRPs are shown by red arrows in f and m.

PR tip, stele, LRP and the tip and base of LR (Fig. 1j-p). As predicted for a transcription factor, *ERF109* was localized in nuclei (Supplementary Fig. 3).

***ERF109* regulates LR development in response to MeJA.** To study the function of *ERF109* in root development, we identified a loss-of-function mutant *erf109* and generated 35S-*ERF109* transgenic lines (Supplementary Fig. 4). The LRP of the wild-type (Col-0), *erf109* and 35S-*ERF109* lines were subsequently examined and quantified. In this study, LRP were counted on the basis of expression of the DR5-GUS marker gene. As shown in Fig. 2a,b, *erf109* had fewer LRP per unit root length than wild type under normal conditions. In contrast, the number of LRP in 35S-*ERF109*-1 was significantly increased. Similarly, we observed additional transgenic lines of 35S-*ERF109*, which showed shorter PRs and more LR than wild type (Supplementary Fig. 5).

To examine the response of roots to MeJA, we transferred 3-day-old seedlings to MS medium without or with MeJA and grown vertically. The PR length of *erf109* was not different from that of wild type. However, the PR length of 35S-*ERF109*-1 was significantly reduced (Fig. 2c,e). Treatment with 10 nM MeJA did not affect the PR length of *erf109*, wild type and 35S-*ERF109*-1

(Fig. 2d,f). We also included an *asa1* mutant in the experiment and examined the dose response of *erf109*, wild type, 35S-*ERF109*-1, 35S-*ERF109*-2 and *asa1* for PR elongation at higher concentrations of MeJA. The *erf109*, wild type and *asa1* showed similar PR response to all tested concentrations of exogenous MeJA (Supplementary Fig. 6).

LR number in wild type, *erf109* and 35S-*ERF109*-1 grown on MS medium was also counted. The *erf109* mutant had a similar number of LR as wild type. However, 35S-*ERF109*-1 had significantly more LR (Fig. 2c,g). In response to 10 nM MeJA treatment, wild type showed increased number of LR but not *erf109* (Fig. 2d,h). These results strongly indicate that *ERF109* has a positive role in LR formation. We also examined MeJA dose response of *erf109*, wild type, 35S-*ERF109*-1, 35S-*ERF109*-2 and *asa1* for LR formation. The *erf109* and *asa1* mutants show less LR formation than wild type under a range dose of MeJA (Supplementary Fig. 7).

The phenotypes of *erf109*, wild type and 35S-*ERF109*-1 in response to salt stress were observed subsequently (Supplementary Fig. 8). LR development was induced by salt treatment. This induction was reduced in *erf109* under 150 mM salt treatment.

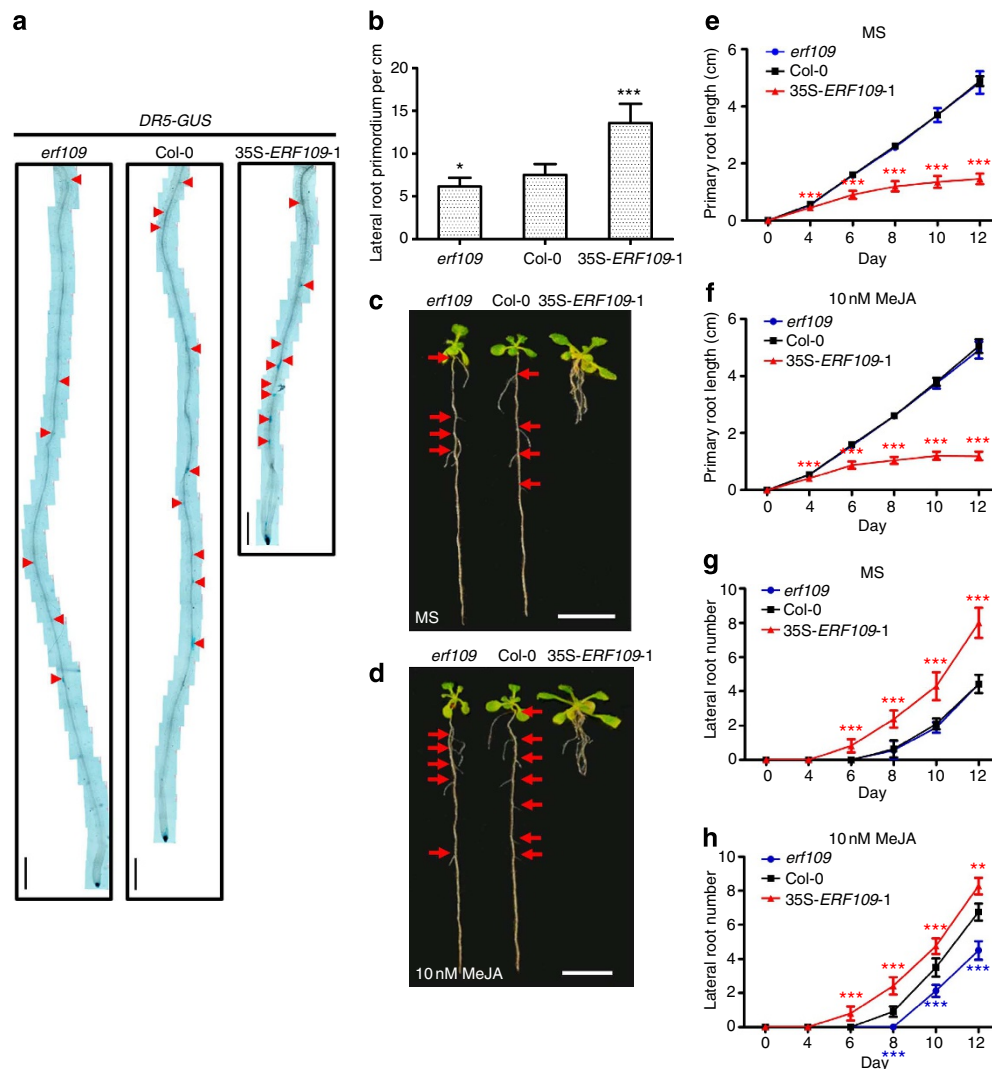


Figure 2 | *ERF109* regulates LRP development in response to MeJA. (a) *erf109* had fewer LRP and 35S-*ERF109-1* had more LRP than the wild type. The locations of LRPs were indicated by red triangles. Scale bar, 0.5 mm. (b) The numbers of LRPs of 5-day-old wild-type, *erf109* and 35S-*ERF109-1* seedlings were counted. Values are mean \pm s.d. ($n=10$ seedlings, $*P<0.05$, $***P<0.001$). Asterisks indicate Student's *t*-test significant differences. (c,d) The root phenotypes of the wild-type, *erf109* and 35S-*ERF109-1* seedlings grown on MS without (c) or with 10 nM MeJA (d). The locations of LRPs were indicated by red arrows. Scale bar, 1 cm. (e,f) PR elongation of the wild-type, *erf109* and 35S-*ERF109-1* seedlings grown on MS without (e) or with 10 nM MeJA (f) were measured at the indicated time points. Values are mean \pm s.d. ($n=25$ seedlings, $***P<0.001$). Asterisks indicate Student's *t*-test significant differences. In (e–g), the *erf109* and Col-0 data overlap so heavily that they are difficult to distinguish. (g,h) The numbers of LRPs of the wild-type, *erf109* and 35S-*ERF109-1* seedlings grown on MS without (g) or with 10 nM MeJA (h) were counted at the indicated time points. Values are mean \pm s.d. ($n=25$ seedlings, $***P<0.001$). Asterisks indicate Student's *t*-test significant differences.

To demonstrate whether the observed phenotypes were caused by *ERF109*, *erf109* was complemented by a 35S-*ERF109* cDNA construct. A line with similar expression level of *ERF109* to that in wild type was used to test for functional complementation (FC) and observation of LR formation (Supplementary Fig. 9a). Consistent with previous results, the *erf109* had fewer LRP than wild type, while the number of LRP of FC (FC-27) was not different from that of wild type (Supplementary Fig. 9b). In addition, consistent with wild type, FC also showed increased LR formation in comparison with *erf109* under 10 nM MeJA treatment (Supplementary Fig. 9c,d).

To confirm this, we analysed additional FC lines with various expression levels of *ERF109* and found that FC lines with high transgene expression showed similar phenotypes as the 35S-*ERF109* (Supplementary Fig. 10). These results further indicate that *ERF109* has a positive role in LR formation.

35S-*ERF109* lines show auxin overproduction phenotypes. In addition to the short PRs and increased numbers of LRP and LR, 35S-*ERF109-1* and 35S-*ERF109-2* had other phenotypes typical of elevated auxin level, such as long hypocotyl, much longer and more root hair (Fig. 3a–c). Mature leaves of 35S-*ERF109-1* were longer, narrower and curled downward with longer petioles compared with those of the wild type (Fig. 3d). These phenotypes are similar to those caused by elevated auxin levels as previously reported¹⁴. These results suggest that *ERF109* might upregulate auxin biosynthesis.

***ERF109* elevates auxin level.** To investigate whether *ERF109* indeed upregulates auxin level, we measured endogenous free IAA contents with liquid chromatography–tandem mass spectrometry system in wild-type, *erf109* and 35S-*ERF109-1* seedlings.

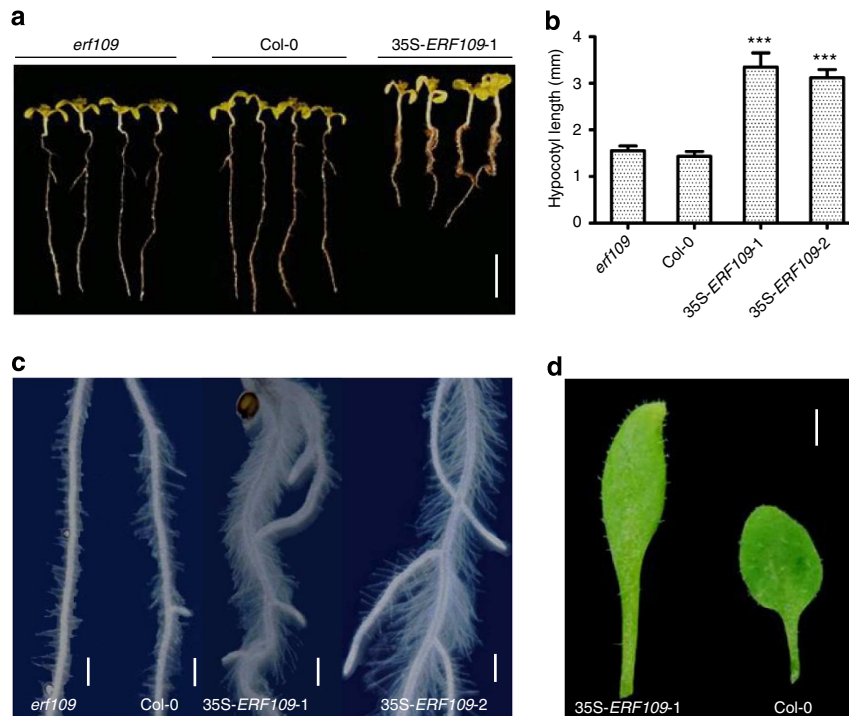


Figure 3 | Auxin overproduction phenotypes of 35S-ERF109 plants. (a) 35S-ERF109-1 seedlings had longer hypocotyls than wild type. Scale bar, 0.5 cm. (b) Hypocotyl elongation of the wild-type, *erf109* 35S-ERF109-1 and 35S-ERF109-2 seedlings grown on MS were measured at the indicated time points. Values are mean \pm s.d. ($n=10$ seedlings, $***P<0.001$). Asterisks indicate Student's *t*-test significant differences. (c) Root hair of the wild-type, *erf109*, 35S-ERF109-1 and 35S-ERF109-2 seedlings. Scale bar, 0.5 mm. (d) Mature leaves of the wild-type and 35S-ERF109-1 seedlings. Scale bar, 2 mm.

As shown in Fig. 4a, auxin levels in the shoot and root tissues of *erf109* were reduced compared with that of the wild type. In contrast, 35S-ERF109-1 had significantly higher auxin levels in both shoot and root tissues than the wild type. Consistent with these results, the expression of the marker genes involved in auxin-dependent signalling processes related to LR development was also affected (Fig. 4b–d). The expressions of *IAA14* (At4g14550) and *IAA19* (At3g15540) were downregulated in the shoot tissue of 35S-ERF109-1. The *erf109* had lower levels of *LBD16* (At2g42430) transcript in both shoot and root tissues than wild type, while the opposite results were observed in 35S-ERF109-1. The altered expression of these genes was consistent with the root phenotypes and auxin levels of wild type, *erf109* and 35S-ERF109. JA-induced *ERF109* enhanced auxin biosynthesis to regulate *Arabidopsis* root architecture.

DR5-GUS reporter was introduced into wild type, *erf109* and 35S-ERF109-1 backgrounds. In the *erf109* background, GUS staining in shoot tissue was weaker than that in wild type. In contrast, the shoot tissue of 35S-ERF109-1 was strongly stained as compared with wild type (Fig. 5a). In root tissues, *DR5-GUS* expression in PR tips was weaker in *erf109* and stronger in 35S-ERF109-1 than that of wild type (Fig. 5a). 35S-ERF109-1 also had elevated expression levels of *DR5-GUS* in the LRP tips at different developmental stages and the LR tips as compared with wild type, while *erf109* had lower levels than wild type (Fig. 5b).

ERF109 regulates the transcription of *ASA1* and *YUC2*.

To identify downstream targets of ERF109, we searched for GCC-boxes in the promoters of auxin biosynthesis and transport genes and found that both *ASA1* and *YUC2* contained one GCC-box in their promoters. To find out whether ERF109 can directly activate the transcriptions of *ASA1* and *YUC2*, we first performed quantitative RT-PCR analysis using wild type, *erf109*

and 35S-ERF109-1 seedlings divided into shoot and root tissues. The data showed that both the candidate target genes could be downregulated in the shoot and root tissues of *erf109* and upregulated in 35S-ERF109-1 (Fig. 6a).

Subsequently, we conducted yeast-one-hybrid assay to determine if ERF109 could directly bind to the GCC-boxes in the promoters of *ASA1* and *YUC2*. The results showed that ERF109 was able to bind to the GCC-boxes in the promoters of *ASA1* and *YUC2* in yeast cells (Fig. 6b,c).

To determine whether ERF109 can directly bind *in vitro* to the GCC-boxes in the promoters of *ASA1* and *YUC2*, we conducted electrophoretic mobility shift assay (EMSA) with GST-ERF109 fusion protein expressed in *E. coli*. As shown in Fig. 6d, the GST-ERF109 fusion protein was able to directly bind to the DNA probes containing the 5'-GCCGCC-3' motif as in the *ASA1* and *YUC2* promoters. The binding was specific as demonstrated by competition assay using unlabelled (competitor) and mutated probes (non-competitor).

To confirm whether the interaction between ERF109 and the GCC-boxes of *ASA1* and *YUC2* promoters takes place *in vivo*, we performed chromatin immunoprecipitation (ChIP) assays using the transgenic plants expressing 35S-haemagglutinin (HA)-ERF109 with similar phenotypes to 35S-ERF109 plants and anti-HA antibodies. As shown in Fig. 6e–g, the *ASA1* and *YUC2* promoter regions containing the GCC-boxes were significantly enriched by ERF109. Thus, the specific binding of ERF109 to the GCC-boxes in the promoters of *ASA1* and *YUC2* was confirmed in *Arabidopsis*.

To visualize the altered spatiotemporal expression patterns of *ASA1* and *YUC2* by ERF109 in *Arabidopsis*, the *ASA1pro-GUS* and *YUC2pro-GUS* reporters were introduced into wild type, *erf109* and 35S-ERF109-1 background by crossing. We first examined the response of *ASA1pro-GUS* and *YUC2pro-GUS* reporter to MeJA treatment in different *ERF109* background.

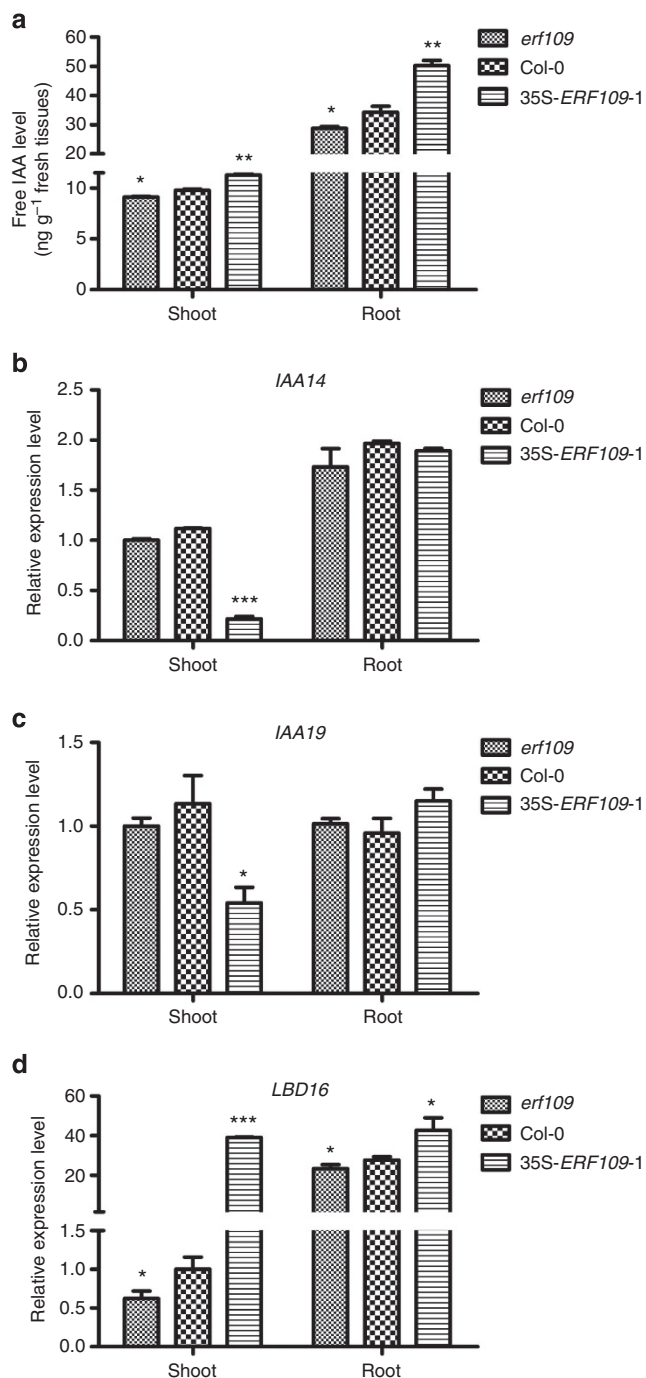


Figure 4 | *ERF109* elevates auxin level in *Arabidopsis*. (a) Free IAA concentration in shoot and root of the wild-type, *erf109* and 35S-*ERF109-1* seedlings. Two-week-old seedlings were divided into shoots and roots for IAA measurements using LC-MS. Values are mean \pm s.e. (four biological repeats, $*P < 0.05$, $**P < 0.01$). Asterisks indicate Student's *t*-test significant differences. (b-d) Quantitative RT-PCR analysis of the marker genes involved in auxin-dependent signalling processes. RNA was isolated from the shoots and roots of two-week-old seedlings of the wild-type, *erf109* and 35S-*ERF109-1*. Values are mean \pm s.d. ($n = 3$ experiments, $*P < 0.05$, $***P < 0.001$). Asterisks indicate Student's *t*-test significant differences.

Without exogenous MeJA treatment, the expression level of *ASA1* and *YUC2* was slightly lower in the root tissues of *erf109* than that in wild type. In response to 10 nM MeJA treatment for 0.5 h, the expression of *ASA1* and *YUC2* was elevated in the root of the wild type. However, it was not affected in *erf109* root under the same

MeJA treatment (Fig. 7a,b). In the 35S-*ERF109-1* background, the expression of *ASA1* and *YUC2* did not show significant difference to MeJA treatment due to the high level expression of *ERF109* from the 35S promoter, which likely overshadowed the JA-induced expression of *ERF109*.

We then examined the expression of *ASA1pro-GUS* and *YUC2pro-GUS* reporter in different tissues in different *ERF109* background. Either in 5- or 10-day-old seedlings, *ASA1pro-GUS* reporter was highly activated in cotyledons and roots in 35S-*ERF109-1* background compared with that in the wild type (Fig. 7c,d). In *erf109* background, its expression level was slightly lower than that in the wild type (Fig. 7c,d). This was more evident in the closer examination of root tip (Fig. 7e-g), maturation zone (Fig. 7h-j) and the region with LRP (Fig. 7k-m). The higher expression level of *ASA1pro-GUS* was observed in the root tips and stele in 35S-*ERF109-1* background and the lowest level in *erf109* background (Fig. 7e-m). The expression of *YUC2pro-GUS* reporter was very similar to that of *ASA1pro-GUS* (Fig. 7n-x) except that GUS staining was hardly visible in the root tips.

The GUS staining results also showed that *ERF109*, *ASA1* and *YUC2* had common expression patterns (Figs 1 and 7 and Supplementary Fig. 2). The results agree with the binding between *ERF109* and the GCC-box in the promoters of *ASA1* and *YUC2*.

To confirm further that *YUC2* is the target of *ERF109*, we introduced 35S-*ERF109* into *yuc2* mutant background by crossing 35S-*ERF109-1* with *yuc2*. The genetic assay showed that the root phenotype of 35S-*ERF109-1 yuc2* was intermediate between 35S-*ERF109-1* and *yuc2* (Fig. 8), which demonstrates that *YUC2* is one of the targets of *ERF109* and suggests that *ERF109* also affects PR length and LR number through other unidentified targets.

Discussion

It is well known that exogenous application of JA dramatically alters root system architecture. Yet the mechanism by which endogenous JA regulates root development remains poorly understood. An endogenous hormone, JA can be generated in response to various environmental stimuli. JA production can also be induced by ectopic expression of transcriptional regulators such as EDT1/HDG11 that activate JA biosynthesis genes, contributing to an improved root system^{31,40}.

JA is known to activate several types of transcription factors and mediate different responses to biotic and abiotic stresses. A number of transcription factors involved in JA signalling, plant defence and wounding response were identified via genome-wide screen and microarray analysis^{35,41}. Transcription factors that respond to JA belong to several large gene families, including ERF, basic Leucine Zipper (bZIP), MYB, MYC and WRKY families⁴². MYC transcription factors are conserved in dicotyledonous plants, and have an important role in JA-mediated regulation of defence and wound-responsive genes^{43,44}. Members of the ERF family, such as *ERF1*, act as integrators of JA and ethylene signalling in the ethylene/JA-dependent defence response⁴⁵. The members of WRKY family, such as *WRKY18*, regulate JA-responsive gene expression^{45,46}. The JA-inducible transcription factors also include MYB family members, such as *MYB24* (refs 35,45,47). Most of these JA-inducible transcription factors act in wound or defence signalling. However, a few JA-responsive transcription factors have been reported to be involved in root development. In this study, we revealed the function of *ERF109* in LR formation.

ERF109 encodes a member of the B-3 group of the ERF/AP2 transcription factor superfamily with a wide variety of functions in plant growth and development as well as environmental signal

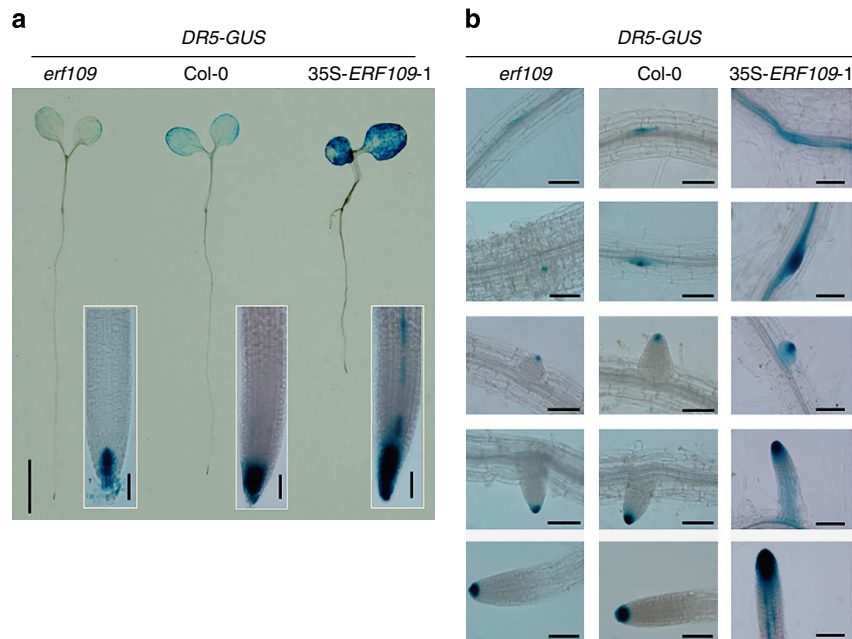


Figure 5 | Altered expression of *DR5-GUS* marker in varied *ERF109* backgrounds. (a) *DR5-GUS* expression levels in 5-day-old *erf109*, wild-type and 35S-*ERF109-1* seedlings. Scale bar, 0.2 cm. *DR5-GUS* expression levels in the PR tips of 7-day-old *erf109*, wild type and 35S-*ERF109-1* seedlings were shown next to the seedlings. Scale bar, 50 μ m. (b) The comparison of *DR5-GUS* expression levels in the initiation sites of LRP, LRPs and LR tips between two-week-old *erf109*, wild type and 35S-*ERF109-1*. Scale bar, 100 μ m.

transduction⁴⁸. Alignment of the deduced ERF109 protein sequence showed that it has low homology with other members of the superfamily and only limited homology within the AP2 domain, suggesting that ERF109 may have a unique role(s) without genetic redundancy to other *ERF* family members. Indeed, we have shown that *ERF109*-mediated cross-talk of JA signalling and auxin to regulate LR formation by directly activating the auxin biosynthesis genes *ASA1* and *YUC2*. Despite that several transcription factors can regulate *YUC* gene expression to affect certain developmental processes⁴⁹, JA-inducible transcription factors-mediated *YUC* expression is yet to be reported. The transcription factors that regulate *ASA1* have not been identified, except for *MYB34/alterred tryptophan regulation 1 (ATR1)* that activates tryptophan gene expression in *Arabidopsis*⁵⁰. Taken together, our finding that *YUC2* and *ASA1* are regulated by ERF109 to affect root development was unexpected.

The transcript levels of *ASA1* and *YUC2* were reduced in *erf109* mutants compared with wild type (Fig. 6a). Reporter gene analyses also showed slight differences in expression levels of *ASA1* and *YUC2* between wild type and *erf109* (Fig. 7). Furthermore, the auxin level of *erf109* plants was reduced (Figs 4a and 5). In addition, *ERF109*, *ASA1* and *YUC2* shared similar expression patterns (Figs 1 and 7 and Supplementary Fig. 2). We provide multiple lines of supporting evidence including yeast-one-hybrid, EMSA and ChIP assays, as well as the genetic analysis that established the interaction between ERF109 and the promoters of both *ASA1* and *YUC2* genes (Figs 6 and 7). The native promoter of *ERF109* was initially used for ChIP assay without success, which was probably due to low expression level of *ERF109*, and has been similarly noted for other transcription factors with low expression⁵¹. However, when we used a stronger promoter, the results showed that *ASA1* and *YUC2* were targets of ERF109.

The *erf109* mutant did not show a significant phenotype of root architecture, which may be explained as follows. First, *ERF109* had very low expression in root tissue under normal growth

conditions, which may reflect the less important role of JA signalling in root development in the absence of environmental stress and the specificity ERF109 for JA signalling in root development. Second, although ERF109 is able to change the auxin content within the root to affect root architecture, the auxin biosynthesis process is a complex metabolic network with multiple biosynthetic routes, and auxin biosynthesis is regulated by many genes with a high level of functional redundancy. Therefore, elimination of *ERF109* may have minimally impacted auxin biosynthesis and root development.

As shown in Fig. 2a,b, 5-day-old *erf109* seedlings had fewer LRP per unit root length than wild type under control conditions, which implies that LRP initiation was either delayed or reduced. However, the lower number of LRP was not reflected in a significant difference in the observed number of LR (Fig. 2g and Supplementary Fig. 7a). We believe that the lack of a significant difference in the number of LR in our assays may be due to the developmental time lag between LRP formation and LR emergence. Assuming a similar rate of LR emergence, we believe that there was insufficient time in our seedling growth assays for the small difference in the number of LRP to cause a significant difference in the number of LR.

ERF109 overexpression lines had elevated IAA levels in both shoot and root tissues in comparison to wild type (Figs 4a and 5), whereas the expression levels of *IAA14* and *IAA19* were lower in the shoot tissues (Fig. 4b,c). *AUX/IAAs* genes are auxin-inducible and the response of most *AUX/IAAs* to IAA is rapid, tissue-specific and dose dependent⁵². In this situation, however, the constitutively elevated IAA levels in *ERF109* overexpressors may have inhibited steady-state mRNA accumulation of *AUX/IAAs* resulting in a different response to what is commonly observed from short-term exogenous IAA treatments.

The reduction in LR formation in *asa1* is much larger than the reduction in *erf109* under MeJA treatment (Supplementary Fig. 7). *ASA1* is a downstream target of ERF109. The expression of *ASA1* was downregulated in *erf109* (Fig. 6a) while it was null in *asa1* (CS16398) mutant (Supplementary Fig. 6j). A higher level of

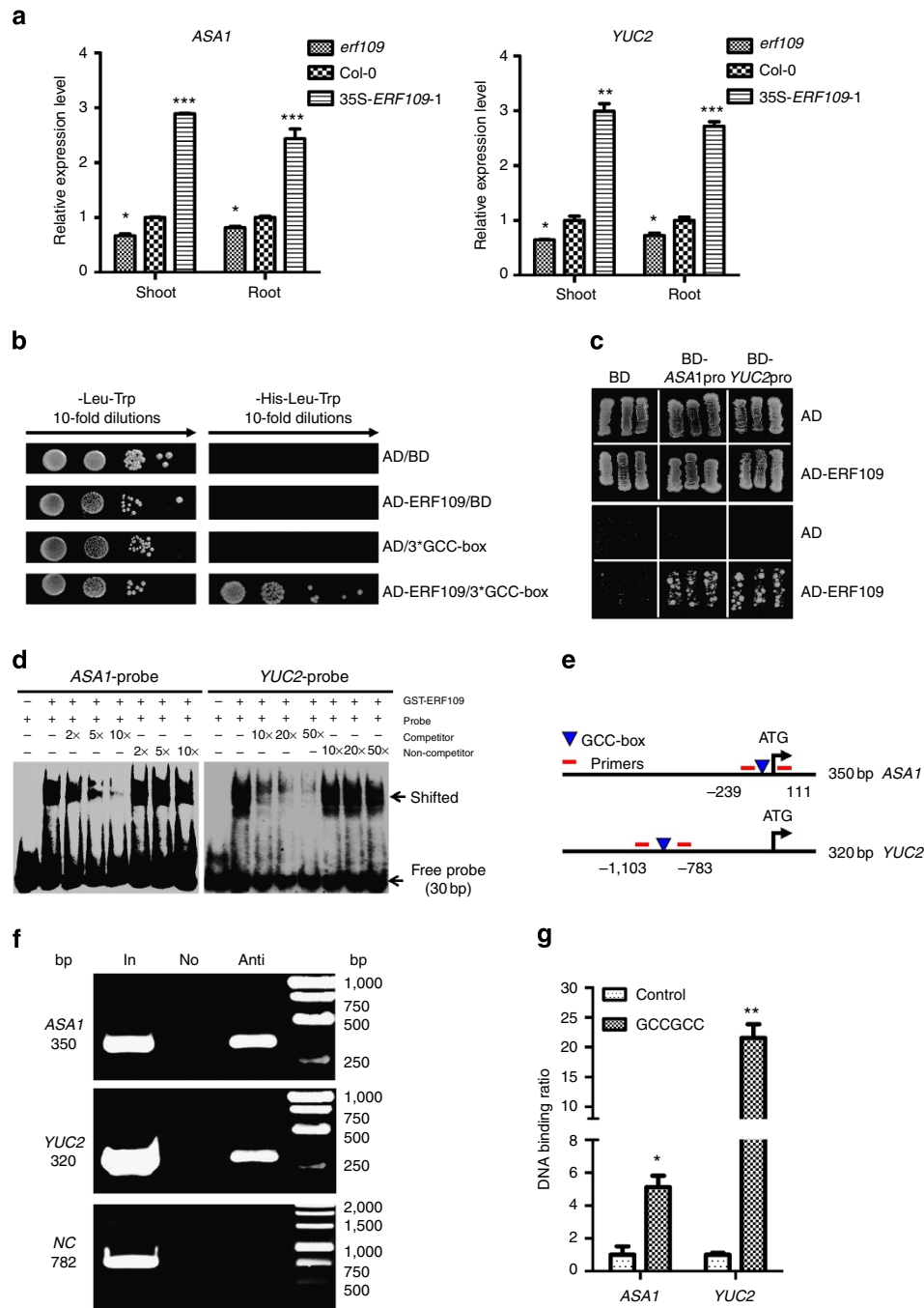


Figure 6 | ERF109 directly regulates the transcriptions of ASA1 and YUC2. (a) Quantitative RT-PCR analysis of transcriptions of ASA1 and YUC2. The shoots and roots of two-week-old *erf109*, wild-type and 35S-ERF109-1 seedlings were used. Values are mean \pm s.d. ($n = 3$ experiments, $**P < 0.01$, $***P < 0.001$). Asterisks indicate Student's *t*-test significant differences. (b) Yeast one-hybrid assay for ERF109 binding to the fragment containing three copies of core sequence of GCC-box in tandem repeat. A serial yeast dilutions (1:1, 1:10, 1:100 and 1:1,000) were grown on SD medium lacking Leu and Trp, and the same medium lacking Leu, Trp and His. The empty pAD and pHis2 vectors were used as negative control. (c) Yeast one-hybrid assay for ERF109 binding to two 30 bp sequences containing the GCC-boxes from the promoter of ASA1 or YUC2, respectively. The six panels on the top showed that yeast were grown on SD medium (-Leu-Trp), and the six panels on the bottom indicated that yeast were grown on SD medium (-His-Leu-Trp). (d) EMSA. Unlabelled probes were used as competitors and mutated probes were used as non-competitors. ERF109-dependent mobility shifts were detected and unlabelled probe competed in a dose-dependent manner while the non-competitor probe did not. (e) The schematic illustration of the locations of GCC-boxes (inverted triangles) in the promoters of ASA1 and YUC2 and the primers used for RT-PCR and quantitative RT-PCR (short lines). (f, g). ChIP assay. About 300 bp ASA1 and YUC2 promoter fragments containing GCC-boxes were enriched by anti-HA antibodies in RT-PCR analysis (f). The region of *tubulin8* (*TUB8*, At5g23860) that do not contain a GCC-box was used as a negative control. In (Input), the chromatin DNA was used as the template; No, ChIP with no antibody was used as the template for negative control; Anti, ChIP with anti-HA antibody was used as the template. M, DNA size marker. The results of ChIP-PCR were confirmed by quantitative RT-PCR (g). The regions of ASA1 and YUC2 that do not contain GCC-box were used as negative controls. Values are mean \pm s.d. ($n = 3$ experiments, $*P < 0.05$, $**P < 0.01$). Asterisks indicate Student's *t*-test significant differences.

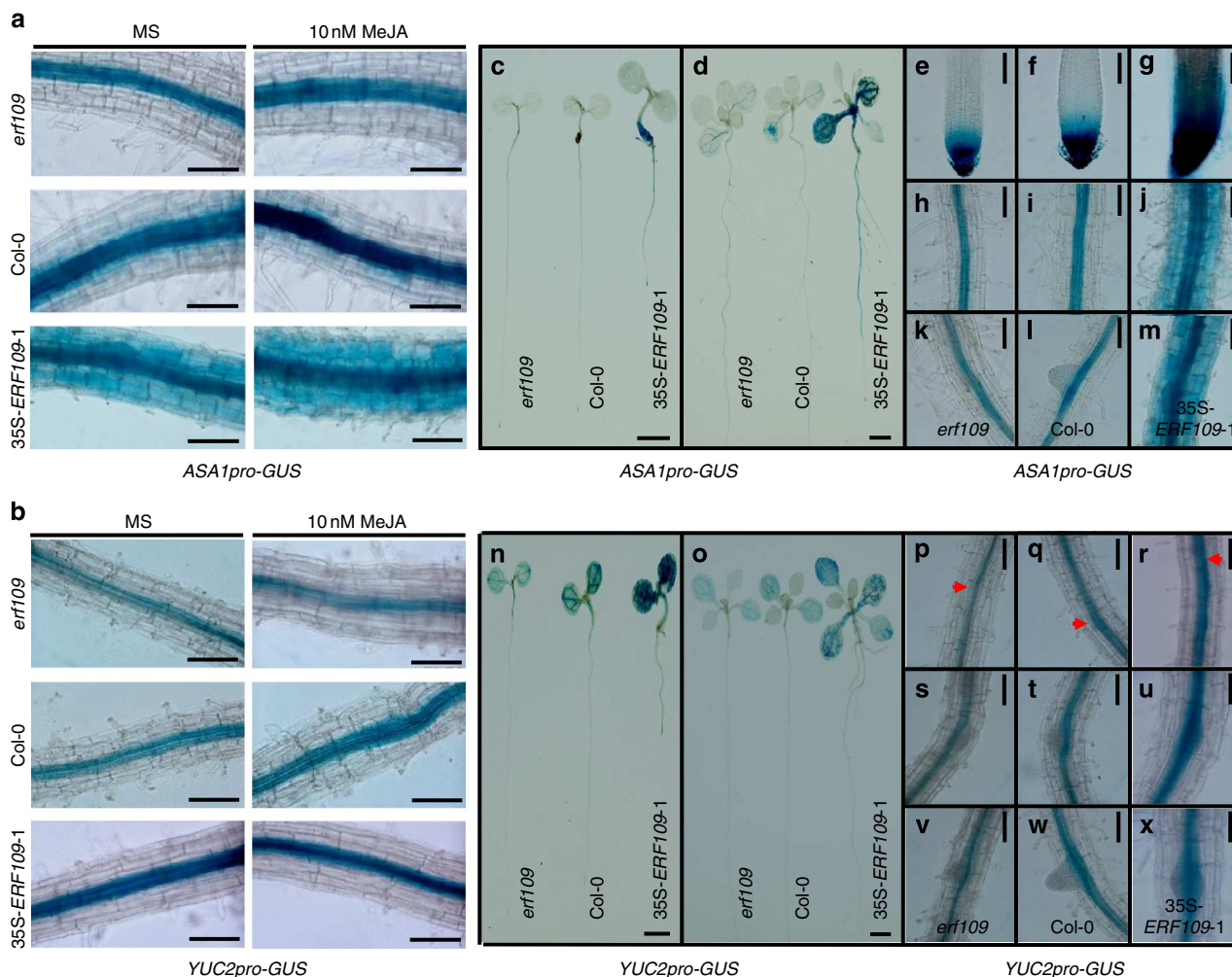


Figure 7 | Altered expression of *ASA1pro-GUS* and *YUC2pro-GUS* in varied *ERF109* genetic backgrounds. (a,b) The expression of either *ASA1pro-GUS* or *YUC2pro-GUS* could not be induced by 10 nM MeJA treatment for 0.5 h in *erf109* compared with that in the wild-type. 7-day-old seedlings were transferred to MS without or with 10 nM MeJA for 0.5 h before GUS staining. Scale bar, 100 μ m. (c–m) The expression levels of *ASA1pro-GUS* in both the shoot and root tissues of *erf109*, wild type and *35S-ERF109-1*. The GUS staining in the shoot tissues were observed using 5-day-old (c) and 10-day-old seedlings (d). Scale bar, 0.2 cm. The GUS staining in the PR tip (e–g), stele of maturation zone (h–j) and the LRP (k–m) were observed using 7-day-old *erf109*, wild-type and *35S-ERF109-1* seedlings. Scale bar, 100 μ m. (n–x) The expression levels of *YUC2pro-GUS* in both the shoot and root tissues of *erf109*, wild type and *35S-ERF109-1*. The expression levels of *YUC2pro-GUS* in the shoot tissues were observed using 5-day-old (n) and 10-day-old seedlings (o). Scale bar, 0.2 cm. The expressions of *YUC2pro-GUS* in the root tissues of 7-day-old *erf109*, wild type and *35S-ERF109-1* were observed (p–x). GUS staining was compared in the stele of maturation zone with LRP at the same developmental stages (early LRP, p–r, the locations of LRPs were shown using red arrows; middle LRP, s–u; and late LRP, v–x). Scale bar, 100 μ m.

ASA1 expression in *erf109* would contribute to the lower reduction in LR formation compared with that in *asal* mutant. In addition, other molecular mechanisms may also be involved in transcriptional regulation of *ASA1* and the response of *ASA1* to JA. Reduced LR formation in *erf109* mutants in response to salt stress suggests that *ERF109* has a function in salt-induced LR development (Supplementary Fig. 8). In addition, the weak response of *ERF109* to SA and ACC indicates that *ERF109* may have a part in cross-talk between SA and IAA, as well as between ethylene and IAA pathways.

We also analysed all possible JA-responsive elements in the promoters of *ASA1* and *YUC2* to identify other transcription factors that may regulate the expression of *ASA1* and *YUC2*, and many JA-responsive elements were identified. In the *YUC2* promoter, one T/G-box (5'-AACGTG-3'), close to the GCC-box, was found. The result implies that there may be other transcription factor(s) involved in the expression of *YUC2* in response to JA. In addition, several 5'-GAGTA-3'

motifs were found in both *ASA1* and *YUC2* promoters. Whether 5'-GAGTA-3' motifs function in the JA-responsive process is worthy of further study. The identification of several JA-responsive elements in *ASA1* and *YUC2* promoters further indicate the complexity of interplay of JA and auxin and the important role of *ERF109* in mediating JA signals and auxin biosynthesis genes.

JA is endogenously produced in response to a variety of environmental stresses and plants adjust accordingly to activate defence responses and modify development processes for survival. In regulation of root development, JA signalling apparently converges with auxin signalling, the major signalling pathway governing root development⁴⁹. Recent research showed that *ASA1* and *YUCCA* were involved in the root response to MeJA treatment²⁶. Our results demonstrate that *ERF109* acts as an important converging point between JA and auxin signalling pathways by integrating JA signalling into auxin biosynthesis to regulate LR formation.

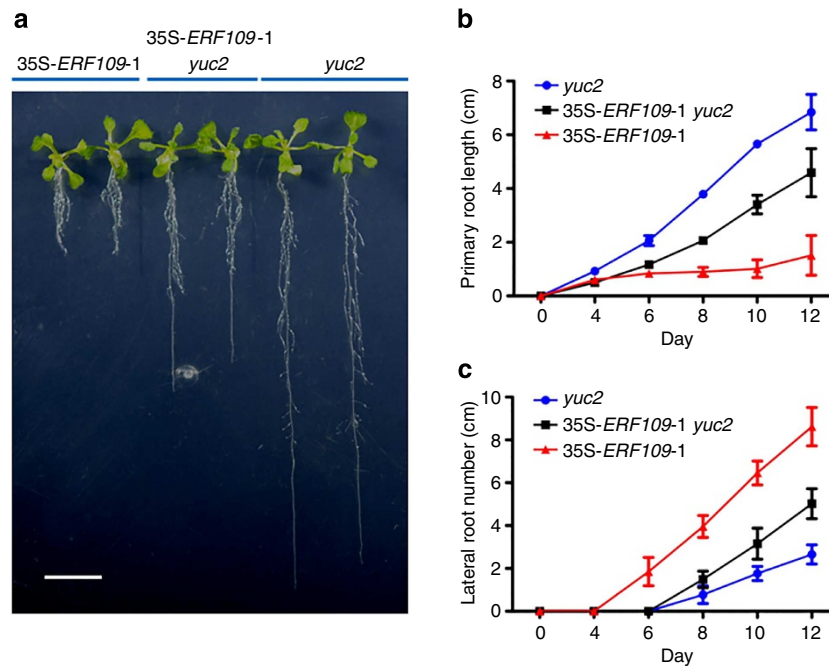


Figure 8 | *YUC2* acts downstream of *ERF109*. (a) The root phenotypes of 35S-*ERF109-1*, 35S-*ERF109-1 yuc2* and *yuc2* seedlings grown on MS. Scale bar, 1 cm. (b) PR elongation of 35S-*ERF109-1*, 35S-*ERF109-1 yuc2* and *yuc2* grown on MS were measured at the indicated time points. Values are mean \pm s.d. ($n = 15$ seedlings). (c) The numbers of LRs of 35S-*ERF109-1*, 35S-*ERF109-1 yuc2* and *yuc2* seedlings grown on MS were counted at the indicated time points. Values are mean \pm s.d. ($n = 15$ seedlings).

On the basis of our results of auxin accumulation (Figs 5 and 7e–g) and no detectable expression of *ERF109* in primary root tip (Fig. 1d,k), it is possible that *ERF109* may affect auxin transport. As a transcription factor, *ERF109* is capable of regulating a suite of target genes. It is possible that some target genes fall into the category of auxin transport. Future transcriptome comparison analyses should help to resolve this.

Methods

Plant materials and growth conditions. The wild type used in our study was *Arabidopsis thaliana* ecotype Columbia-0 (Col-0). A homozygous *erf109* loss-function mutant was identified from Salk_150614, which was ordered from Arabidopsis Biological Resource Center. The *ERF109pro-GUS*, 35S-*ERF109-GFP*, 35S-*ERF109* and 35S-HA-*ERF109* constructs were transformed into Col-0 by *Agrobacterium tumefaciens*-mediated transformation using strain C58C1. For *ERF109pro-GUS*, the promoter of *ERF109* was amplified and cloned into pDONR207 with the primers GUS/*ERF109* P1 and GUS/*ERF109* P2 (Supplementary Table 1), and subsequently shuttled it into the pCB308R vector to construct the GUS fusion vector. For 35S-*ERF109-GFP* used in the transient expression assay, the *ERF109*-coding region was amplified and cloned into pCB2008E vector to construct the GFP fusion vector with the primers 8E/*ERF109* P1 and 8E/*ERF109* P2. To obtain 35S-*ERF109-GFP* transgenic plants, the *ERF109*-coding region was amplified and cloned into pDONR207 with primers pGWB5/*ERF109* P1 and pGWB5/*ERF109* P2, and subsequently shuttled it into pGWB5 vector. For 35S-*ERF109*, the *ERF109*-coding region was amplified and cloned into pDONR207 with primers pCB2004/*ERF109* P1 and pCB2004/*ERF109* P2 and subsequently shuttled it into pCB2004 vector. To make the 35S-HA-*ERF109* construct, which was used for function complementation and ChIP assays, the *ERF109*-coding region was amplified and cloned into pDONR207 with the primers HA-*ERF109* P1 and HA-*ERF109* P2, and subsequently shuttled it into pCB2004 vector. The plant materials *DR5-GUS*²⁹, *YUC2pro-GUS*²⁹ and *ASA1pro-GUS*²⁸ were used as female parents in genetic analysis, while *erf109*, Col-0 and 35S-*ERF109* were used as male parents.

Arabidopsis seeds were surface sterilized for 10 min in 10% bleach and washed five times at least with sterile water. Plant seeds were kept at 4 °C for 2 days in darkness before germination on horizontal agar plates containing solid Murashige and Skoog (MS) medium with 1% (w/v) sucrose at 22 °C under 16-h light/8-h dark cycles. For analysis of PR length and LR number, 3-day-old seedlings were transferred to MS solid mediums without or with MeJA and grown vertically. The PR length of seedlings grown on medium containing the indicated concentrations of MeJA was measured and the number of LR were counted at the indicated time points. For the detection of transcript level of *ERF109* under

different hormone and stress treatments, the seedlings were grown on MS medium vertically at first. Then, the 7-day-old or 14-day-old seedlings were transferred to MS medium without (control) or with different hormones or compounds for 0.5 h before RNA extraction or GUS staining.

Agrobacterium-mediated transformation of Arabidopsis. The constructs were electroporated into *Agrobacterium tumefaciens* C58C1 and transferred into *Arabidopsis* using the floral-dip method⁵³. *Agrobacterium* cells containing the appropriate construct were collected by centrifugation. *Agrobacterium* cells were resuspended using 5% (w/v) sucrose solution until the OD₆₀₀ of *Agrobacterium* cell suspension was 0.8. Silwet L-77, as a strong surfactant, was added to the sucrose solution to obtain a final concentration of 0.05% (v/v). *Agrobacterium* cell suspension was transferred to the glass dish. Developing *Arabidopsis* inflorescences were dipped into *Agrobacterium* cell suspension for about 10 s. The transformed plants were grown in darkness horizontally for 16–24 h. The seeds of treated plants were harvested after *Agrobacterium*-mediated transformation. The seedlings of transformants were obtained by glufosinate or kanamycin screening.

Subcellular localization assay. For transient expression assay, the *ERF109*-coding region was amplified and cloned into the vector pCB2008E to construct the GFP fusion vector⁵⁴. The inserted sequence was confirmed by sequencing. Then the construct was delivered into the onion epidermal cells via microprojectile bombardment of particle gun. The *ERF109*-coding region was also cloned into pGWB5 and the construct was transferred into Col-0 to create transgenic plants.

The fluorescence of GFP in onion epidermal cells and the root tissues of transgenic plants were observed under a fluorescence microscope (ZEISS Axio skop2 plus).

Analysis of GUS activity. The promoter of *ERF109* was amplified and cloned into pCB308R (ref. 54). Then the construct was transferred into Col-0. Histochemical staining for GUS activity in *Arabidopsis* was performed using the T2 population⁵⁵. The *Arabidopsis* seedlings or various tissues were incubated in GUS staining solution containing 0.5 mg ml⁻¹ 5-bromo-4-chloro-3-indolyl-l-b-D-glucuronide cyclohexylamine salt (X-Gluc), 0.1 M sodium phosphate buffer (pH 7.0), 0.5 mM potassium ferricyanide, 0.5 mM potassium ferrocyanide and 0.1% Triton X-100 at 37 °C. Experimental materials were subsequently de-stained and stored in 70% ethanol. The results were observed using a light microscope with a camera (HIROX).

Gene expression analysis. Total RNA was isolated from various tissues as indicated by the TRIZOL reagent (Invitrogen). The reverse transcription reaction, which was used as template for PCR amplification, was carried out with Prime

Script RT reagent Kit (TaKaRa). For RT-PCR analysis, the PCR products were examined on a 1 or 2% agarose gel stained with ethidium bromide. For quantitative RT-PCR analysis, PCR was carried out on a Step One Real-Time PCR system (Applied Biosystems) with the SYBR green (SYBR Premix Ex Taq II, TaKaRa). The transcript levels of target genes were examined using specific primers (Supplementary Table 1). *Ubiquitin5* (*UBQ5*, At3g62250) was used as the internal control.

Identification of *erf109* and transgenic plants of *ERF109*. Homozygous T-DNA insertion mutants of Salk_150614 were identified using genomic PCR with specific primers and the T-DNA primer Lbb1 (Supplementary Table 1)⁵⁶. RT-PCR and quantitative RT-PCR were performed to confirm the results of genomic PCR screen with specific primers (Supplementary Table 1). 35S-*ERF109* and FC line were obtained by glufosinate screening and then they were identified by quantitative RT-PCR.

Free IAA measurement. Free IAA measurement of shoot tissues and root tissues of Col-0, *erf109* and 35S-*ERF109* seedlings. The *Arabidopsis* seedlings of Col-0, *erf109* and 35S-*ERF109* were grown on MS medium containing 1% sucrose. Two-week-old seedlings were divided into shoot tissues and root tissues. Each plant tissue was collected, quickly frozen in liquid nitrogen and ground into a fine powder (200 mg). ³H-IAA (CDN isotopes) was used as internal standard. Shoot and root tissues were homogenized and extracted for 24 h in methanol containing internal standard. Purification was performed using Oasis Max solid phase extract cartridge (Waters) after centrifugation. IAA measurement was carried out with a liquid chromatography-tandem mass spectrometry system consisted of an Acquity Ultra Performance Liquid Chromatography (Acquity UPLC; Waters) and a triple quadrupole tandem mass spectrometer (QTRAP 5500; AB SCIEX)⁵⁷.

Yeast-one-hybrid assay. Yeast-one-hybrid assay is a powerful technique to rapidly test the interaction between a transcription factor and a regulatory DNA sequence specifically bound by the transcription factor. It was performed using pAD-GAL4-2.1 and the reporter plasmid pHIS2 (ref. 58). Briefly, three copies of GCC-box element in tandem repeat were cloned into the reporter plasmid pHIS2. The *ATERF109* gene was cloned into the plasmid pAD-GAL4-2.1 to produce the effector plasmid pAD/ATERF109. The reporter and effector plasmids were introduced into yeast cells. The transformants were observed for their growth on SD/-Trp-Leu-His medium or this medium plus 3-aminotriazole (3-AT) following the instruction of the BD Matchmaker Library Construction & Screening Kits (www.bdbiosciences.com).

To obtain pAD/ERF109 plasmid, the *ERF109*-coding region was amplified and cloned into the pAD-GAL4-2.1 vector (AD vector) using *Bam*HI and *Xba*I sites with the primers Y1H ERF109 P1 and Y1H ERF109 P2. In pAD/ERF109 plasmid, the *ERF109*-coding region was translationally fused to the GAL4-AD domain to express fusion protein for DNA binding in yeast-one-hybrid assay. Then, three pairs of sequences containing GCC-boxes were synthesized with cohesive ends (Sangon of Shanghai, China) (Supplementary Table 1). Each pair of these sequences was annealed and ligated into the *Sac*I and *Mlu*I sites of the nutritional reporter plasmid pHIS2 (BD vector). The inserted sequences were confirmed by sequencing. The pAD and pHIS2 empty vector were used as negative control.

Different combinations of plasmids were co-transformed into yeast strain Y187 competent cells. Yeast cells were grown on synthetic defined (SD)/-Trp-Leu medium for 3 days at 30°C. Then, yeast cells without or with different dilutions (1:10, 1:100 and 1:1,000) were transferred to SD/-Trp-Leu medium and SD/-Trp-Leu-His medium with 10 mM 3-aminotriazole (3-AT, Sigma), respectively. The yeast cell containing pAD/ERF109 and pHIS2/*cis*-element were grown normally on SD/-Trp-Leu-His medium with 10 mM 3-AT, which indicated the interaction between ERF109 and the corresponding *cis*-element.

Identification of JA-responsive elements. JA-responsive elements in *ASA1* and *YUC2* promoters were screened on the basis of the sequence of G-Box (5'-CAC GTGG-3'), which can be bound by basic Helix-Loop-Helix (bHLH) transcription factors^{59,60}; the hexamer sequence (5'-TGACGT-3') (ref. 61); the JA- and elicitor-responsive element (JERE)⁶²; JASE1 (5'-CGTCAATGAA-3') and JASE2 (5'-CATACGTGCTCAA-3') (ref. 63); the T/G-box (5'-AACGTG-3') and GCC-Box^{64,65}; a duplicated 5'-GAGTA-3' motif⁶⁶; and other JA-responsive motifs reported^{67,68}.

EMSA assay. The GST-ERF109 fusion protein was expressed in *E. coli* strain Rosseta2. 30bp free probes covering GCC-boxes, unlabelled probes (competitor) and mutated probes (non-competitor) carrying 6 bp mutation at GCC-boxes were commercially synthesized (Sangon) as single-stranded (ss) DNA (Supplementary Table 1). Free probes were synthesized and labelled with Digoxigenin (DIG) at the 5' end. In the mutated probes, the sequence 5'-CATTGA-3' replaced the core sequence of GCC-box (5'-GCCGCC-3'). Equal amounts of complementary ssDNA were mixed, 95 °C for 5 min and slowly cooled down to 25 °C. EMSA was performed using a DIG Gel Shift Kit, 2nd Generation (Roche). DIG-labelled probes were incubated in 5 × binding buffer (100 mM Hepes, pH 7.6, 5 mM EDTA,

50 mM (NH₄)₂SO₄, 5 mM DTT, 1% (w/v) Tween 20, 150 mM KCl) with or without GST-ERF109 at room temperature for 20 min. For competition experiments, different amounts of unlabelled and mutated probes were added to the binding reaction. Loading buffer (5 ×) was then added to the binding reaction. Each reaction was loaded on a 4.5% native polyacrylamide gel in 0.5 × TBE buffer. The results were detected using a CCD camera system (Image Quant LAS 4000).

ChIP assay. Ten-day-old 35S-HA-*ERF109* transgenic seedlings and anti-HA antibodies (1:100 for ChIP assay, HA-Tag, 26D11, Mouse mAb, M20003, Abmart, Shanghai, China) were used for ChIP experiments⁶⁹. Briefly, the transgenic seedlings were ground into a fine powder with liquid nitrogen and resuspended in nuclei isolation buffer. The nucleus were then collected by centrifugation and resuspended with nuclei lysis buffer. The resuspended chromatin was sonicated to fragments with various sizes (250 bp–1 kb) subsequently. HA-ERF109 was precipitated from input DNA with anti-HA antibodies or without any antibodies. Protein A agarose beads (Millipore, USA) were added into the incubation mixture for additional 2 h at 4 °C. The immune complexes were eluted from the washed protein A beads. The DNA was purified with phenol/chloroform (1:1, v/v) and precipitated. The purified DNA and input DNA were used as templates. The enrichments of DNA fragments were determined by RT-PCR and quantitative RT-PCR with specific primers (Supplementary Table 1; ref. 70).

Genetic analysis. Crosses were generated by transferring pollen from mature anthers of male parent to the stigmas of previously emasculated flowers of female parent.

References

1. Van Norman, J. M., Xuan, W., Beeckman, T. & Benfey, P. N. To branch or not to branch: the role of pre-patterning in lateral root formation. *Development* **140**, 4301–4310 (2013).
2. Malamy, J. E. Intrinsic and environmental response pathways that regulate root system architecture. *Plant Cell Environ.* **28**, 67–77 (2005).
3. Peret, B. *et al.* Arabidopsis lateral root development: an emerging story. *Trends Plant Sci.* **14**, 399–408 (2009).
4. De Smet, I., Vanneste, S., Inze, D. & Beeckman, T. Lateral root initiation or the birth of a new meristem. *Plant Mol. Biol.* **60**, 871–887 (2006).
5. Lavenus, J. *et al.* Lateral root development in Arabidopsis: fifty shades of auxin. *Trends Plant Sci.* **18**, 450–458 (2013).
6. Fukaki, H. & Tasaka, M. Hormone interactions during lateral root formation. *Plant Mol. Biol.* **69**, 437–449 (2009).
7. Petricka, J. J., Winter, C. M. & Benfey, P. N. Control of Arabidopsis root development. *Annu. Rev. Plant Biol.* **63**, 563–590 (2012).
8. De Smet, I. *et al.* Analyzing lateral root development: how to move forward. *Plant Cell* **24**, 15–20 (2012).
9. Marhavý, P. *et al.* Auxin reflux between the endodermis and pericycle promotes lateral root initiation. *EMBO J.* **32**, 149–158 (2013).
10. Kelley, D. R. & Estelle, M. Ubiquitin-mediated control of plant hormone signaling. *Plant Physiol.* **160**, 47–55 (2012).
11. Calderon Villalobos, L. I. *et al.* A combinatorial TIR1/AFB-Aux/IAA co-receptor system for differential sensing of auxin. *Nat. Chem. Biol.* **8**, 477–485 (2012).
12. Okushima, Y., Fukaki, H., Onoda, M., Theologis, A. & Tasaka, M. ARF7 and ARF19 regulate lateral root formation via direct activation of LBD/ASL genes in Arabidopsis. *Plant Cell* **19**, 118–130 (2007).
13. Goh, T., Joi, S., Mimura, T. & Fukaki, H. The establishment of asymmetry in Arabidopsis lateral root founder cells is regulated by LBD16/ASL18 and related LBD/ASL proteins. *Development* **139**, 883–893 (2012).
14. Zhao, Y. *et al.* A role for flavin monooxygenase-like enzymes in auxin biosynthesis. *Science* **291**, 306–309 (2001).
15. Wolters, H. & Jurgens, G. Survival of the flexible: hormonal growth control and adaptation in plant development. *Nat. Rev. Genet.* **10**, 305–317 (2009).
16. Hoffmann, M., Hentrich, M. & Pollmann, S. Auxin-oxylipin crosstalk: relationship of antagonists. *J. Integr. Plant Biol.* **53**, 429–445 (2011).
17. Benkova, E. & Hejatková, J. Hormone interactions at the root apical meristem. *Plant Mol. Biol.* **69**, 383–396 (2009).
18. Turner, J. G., Ellis, C. & Devoto, A. The jasmonate signal pathway. *Plant Cell* **14**(Suppl): S153–S164 (2002).
19. Wasternack, C. Jasmonates: an update on biosynthesis, signal transduction and action in plant stress response, growth and development. *Ann. Bot.* **100**, 681–697 (2007).
20. Ueda, J. & Kato, J. Isolation and Identification of a Senescence-promoting Substance from Wormwood (*Artemisia absinthium* L.). *Plant Physiol.* **66**, 246–249 (1980).
21. Kazan, K. & Manners, J. M. Jasmonate signaling: toward an integrated view. *Plant Physiol.* **146**, 1459–1468 (2008).
22. Tiryaki, I. & Staswick, P. E. An Arabidopsis mutant defective in jasmonate response is allelic to the auxin-signaling mutant *axr1*. *Plant Physiol.* **130**, 887–894 (2002).

23. Ren, C. *et al.* Point mutations in Arabidopsis Cullin1 reveal its essential role in jasmonate response. *Plant J.* **42**, 514–524 (2005).
24. Pauwels, L. *et al.* NINJA connects the co-repressor TOPLESS to jasmonate signalling. *Nature* **464**, 788–791 (2010).
25. Nagpal, P. *et al.* Auxin response factors ARF6 and ARF8 promote jasmonic acid production and flower maturation. *Development* **132**, 4107–4118 (2005).
26. Hentrich, M. *et al.* The jasmonic acid signaling pathway is linked to auxin homeostasis through the modulation of YUCCA8 and YUCCA9 gene expression. *Plant J.* **74**, 626–637 (2013).
27. Gutierrez, L. *et al.* Auxin controls Arabidopsis adventitious root initiation by regulating jasmonic acid homeostasis. *Plant Cell* **24**, 2515–2527 (2012).
28. Sun, J. *et al.* Arabidopsis ASA1 is important for jasmonate-mediated regulation of auxin biosynthesis and transport during lateral root formation. *Plant Cell* **21**, 1495–1511 (2009).
29. Cheng, Y., Dai, X. & Zhao, Y. Auxin biosynthesis by the YUCCA flavin monooxygenases controls the formation of floral organs and vascular tissues in Arabidopsis. *Genes Dev.* **20**, 1790–1799 (2006).
30. Sun, J. *et al.* Jasmonate modulates endocytosis and plasma membrane accumulation of the Arabidopsis PIN2 protein. *New Phytol.* **191**, 360–375 (2011).
31. Yu, H. *et al.* Activated Expression of an Arabidopsis HD-START Protein Confers Drought Tolerance with Improved Root System and Reduced Stomatal Density. *Plant Cell* **20**, 1134–1151 (2008).
32. Ohme-Takagi, M. & Shinshi, H. Ethylene-inducible DNA binding proteins that interact with an ethylene-responsive element. *Plant Cell* **7**, 173–182 (1995).
33. Hao, D., Ohme-Takagi, M. & Sarai, A. Unique mode of GCC box recognition by the DNA-binding domain of ethylene-responsive element-binding factor (ERF domain) in plant. *J. Biol. Chem.* **273**, 26857–26861 (1998).
34. Riechmann, J. L. & Meyerowitz, E. M. The AP2/EREBP family of plant transcription factors. *Biol. Chem.* **379**, 633–646 (1998).
35. Wang, Z. *et al.* Identification and characterization of COI1-dependent transcription factor genes involved in JA-mediated response to wounding in Arabidopsis plants. *Plant Cell Rep.* **27**, 125–135 (2008).
36. Khandelwal, A., Elvitigala, T., Ghosh, B. & Quatrano, R. S. Arabidopsis transcriptome reveals control circuits regulating redox homeostasis and the role of an AP2 transcription factor. *Plant Physiol.* **148**, 2050–2058 (2008).
37. Xie, D. X., Feys, B. F., James, S., Nieto-Rostro, M. & Turner, J. G. COI1: an Arabidopsis gene required for jasmonate-regulated defense and fertility. *Science* **280**, 1091–1094 (1998).
38. Xu, L. *et al.* The SCF(COI1) ubiquitin-ligase complexes are required for jasmonate response in Arabidopsis. *Plant Cell* **14**, 1919–1935 (2002).
39. Yan, J. *et al.* The Arabidopsis CORONATINE INSENSITIVE1 protein is a jasmonate receptor. *Plant Cell* **21**, 2220–2236 (2009).
40. Yu, L. *et al.* Arabidopsis Enhanced Drought Tolerance1/HOMEODOMAIN GLABROUS11 Confers Drought Tolerance in Transgenic Rice without Yield Penalty. *Plant Physiol.* **162**, 1378–1391 (2013).
41. McGrath, K. C. *et al.* Repressor- and activator-type ethylene response factors functioning in jasmonate signaling and disease resistance identified via a genome-wide screen of Arabidopsis transcription factor gene expression. *Plant Physiol.* **139**, 949–959 (2005).
42. Qu, L. J. & Zhu, Y. X. Transcription factor families in Arabidopsis: major progress and outstanding issues for future research. *Curr. Opin. Plant Biol.* **9**, 544–549 (2006).
43. Niu, Y., Figueroa, P. & Browse, J. Characterization of JAZ-interacting bHLH transcription factors that regulate jasmonate responses in Arabidopsis. *J. Exp. Bot.* **62**, 2143–2154 (2011).
44. Santino, A. *et al.* Jasmonate signaling in plant development and defense response to multiple (a)biotic stresses. *Plant Cell Rep.* **32**, 1085–1098 (2013).
45. Fonseca, S., Chico, J. M. & Solano, R. The jasmonate pathway: the ligand, the receptor and the core signalling module. *Curr. Opin. Plant Biol.* **12**, 539–547 (2009).
46. Xu, X., Chen, C., Fan, B. & Chen, Z. Physical and functional interactions between pathogen-induced Arabidopsis WRKY18, WRKY40, and WRKY60 transcription factors. *Plant Cell* **18**, 1310–1326 (2006).
47. Mandaokar, A. & Browse, J. MYB108 acts together with MYB24 to regulate jasmonate-mediated stamen maturation in Arabidopsis. *Plant Physiol.* **149**, 851–862 (2009).
48. Nakano, T., Suzuki, K., Fujimura, T. & Shinshi, H. Genome-wide analysis of the ERF gene family in Arabidopsis and rice. *Plant Physiol.* **140**, 411–432 (2006).
49. Zhao, Y. Auxin biosynthesis and its role in plant development. *Annu. Rev. Plant Biol.* **61**, 49–64 (2010).
50. Bender, J. & Fink, G. R. A Myb homologue, ATR1, activates tryptophan gene expression in Arabidopsis. *Proc. Natl Acad. Sci. U S A* **95**, 5655–5660 (1998).
51. Xu, P. *et al.* HDG11 upregulates cell-wall-loosening protein genes to promote root elongation in Arabidopsis. *J. Exp. Bot.* **65**, 4285–4295 (2014).
52. Abel, S., Nguyen, M. D. & Theologis, A. The PS-IAA4/5-like family of early auxin-inducible mRNAs in Arabidopsis thaliana. *J. Mol. Biol.* **251**, 533–549 (1995).
53. Bent, A. F. Arabidopsis in planta transformation. Uses, mechanisms, and prospects for transformation of other species. *Plant Physiol.* **124**, 1540–1547 (2000).
54. Lei, Z. Y. *et al.* High-throughput binary vectors for plant gene function analysis. *J. Integr. Plant Biol.* **49**, 556–567 (2007).
55. Jefferson, R. A., Kavanagh, T. A. & Bevan, M. W. Gus Fusions - Beta-Glucuronidase as a Sensitive and Versatile Gene Fusion Marker in Higher-Plants. *EMBO J.* **6**, 3901–3907 (1987).
56. Alonso, J. M. *et al.* Genome-wide insertional mutagenesis of Arabidopsis thaliana. *Science* **301**, 653–657 (2003).
57. Fu, J., Chu, J., Sun, X., Wang, J. & Yan, C. Simple, rapid, and simultaneous assay of multiple carboxyl containing phytohormones in wounded tomatoes by UPLC-MS/MS using single SPE purification and isotope dilution. *Anal. Sci.* **28**, 1081–1087 (2012).
58. Mu, R. L. *et al.* An R2R3-type transcription factor gene AtMYB59 regulates root growth and cell cycle progression in Arabidopsis. *Cell Res.* **19**, 1291–1304 (2009).
59. Kim, S. R., Choi, J. L., Costa, M. A. & An, G. Identification of G-Box Sequence as an Essential Element for Methyl Jasmonate Response of Potato Proteinase Inhibitor II Promoter. *Plant Physiol.* **99**, 627–631 (1992).
60. Hong, G. J., Xue, X. Y., Mao, Y. B., Wang, L. J. & Chen, X. Y. Arabidopsis MYC2 interacts with DELLA proteins in regulating sesquiterpene synthase gene expression. *Plant Cell* **24**, 2635–2648 (2012).
61. Kim, S. R., Kim, Y. & An, G. Identification of methyl jasmonate and salicylic acid response elements from the nopaline synthase (nos) promoter. *Plant Physiol.* **103**, 97–103 (1993).
62. Menke, F. L., Champion, A., Kijne, J. W. & Memelink, J. A novel jasmonate- and elicitor-responsive element in the periwinkle secondary metabolite biosynthetic gene Str interacts with a jasmonate- and elicitor-inducible AP2-domain transcription factor, ORCA2. *EMBO J.* **18**, 4455–4463 (1999).
63. He, Y. & Gan, S. Identical promoter elements are involved in regulation of the OPR1 gene by senescence and jasmonic acid in Arabidopsis. *Plant Mol. Biol.* **47**, 595–605 (2001).
64. Guerineau, F., Benjdia, M. & Zhou, D. X. A jasmonate-responsive element within the A. thaliana vsp1 promoter. *J. Exp. Bot.* **54**, 1153–1162 (2003).
65. Brown, R. L., Kazan, K., McGrath, K. C., Maclean, D. J. & Manners, J. M. A role for the GCC-box in jasmonate-mediated activation of the PDF1.2 gene of Arabidopsis. *Plant Physiol.* **132**, 1020–1032 (2003).
66. Boter, M., Ruiz-Rivero, O., Abdeen, A. & Prat, S. Conserved MYC transcription factors play a key role in jasmonate signaling both in tomato and Arabidopsis. *Genes Dev.* **18**, 1577–1591 (2004).
67. Takeda, S., Sugimoto, K., Otsuki, H. & Hirochika, H. A 13-bp cis-regulatory element in the LTR promoter of the tobacco retrotransposon Tto1 is involved in responsiveness to tissue culture, wounding, methyl jasmonate and fungal elicitors. *Plant J.* **18**, 383–393 (1999).
68. Miyamoto, K. *et al.* Identification of an E-box motif responsible for the expression of jasmonic acid-induced chitinase gene OsChia4a in rice. *J. Plant Physiol.* **169**, 621–627 (2012).
69. Gendrel, A. V., Lippman, Z., Martienssen, R. & Colot, V. Profiling histone modification patterns in plants using genomic tiling microarrays. *Nat. Methods* **2**, 213–218 (2005).
70. Mukhopadhyay, A., Deplancke, B., Walhout, A. J. & Tissenbaum, H. A. Chromatin immunoprecipitation (ChIP) coupled to detection by quantitative real-time PCR to study transcription factor binding to DNA in *Caenorhabditis elegans*. *Nat. Protoc.* **3**, 698–709 (2008).

Acknowledgements

This work was supported by the Chinese Academy of Science (grant no. KSCX3-YW-N-007), the Ministry of Science and Technology of China (grant no. 2012CB114304), and the National Nature Science Foundation of China (grant no. 30830075). The authors thank the Arabidopsis Biological Resource Center for providing the seeds of Salk_150614 and *asa1* (CS16398), Dr Chuanyou Li for providing *ASA1pro-GUS* and *coi1-2* as well as his critical review of the manuscript, Dr Yunde Zhao for providing *YUC2pro-GUS* and his critical review of the manuscript, Dr Jirong Huang for providing pGWBS vector. We thank the expertise of Shuang Fang and Jinfang Chu (National Centre for Plant Gene Research (Beijing), Institute of Genetics and Developmental Biology, Chinese Academy of Sciences, Beijing, China) in determining free IAA contents of *Arabidopsis* and the National Nature Science Foundation of China (grant no. 91117016).

Author contributions

X.-T.C. designed the study, performed the experiments, interpreted the results and wrote the manuscript. P.X. contributed to the identification of Salk_150614 and construction of 35S-*ERF109* vector. P.-X.Z., R.L. and L.-H.Y. participated in the quantitative analysis of the marker genes involved in auxin-dependent signalling processes. C.-B.X. designed the experiments, discussed the results, edited the manuscript and supervised the project.

Additional information

Supplementary Information accompanies this paper at <http://www.nature.com/naturecommunications>

Competing financial interests: The authors declare no competing financial interests.

Reprints and permission information is available online at <http://npg.nature.com/reprintsandpermissions/>

How to cite this article: Cai, X.-T. *et al.* *Arabidopsis* ERF109 mediates cross-talk between jasmonic acid and auxin biosynthesis during lateral root formation. *Nat. Commun.* 5:5833 doi: 10.1038/ncomms6833 (2014).